Article

CRYSTAL GROWTH AND SPECTROSCOPY OF Yb2+ DOPED CsI SINGLE CRYSTAL

Dmitriy Sofich *, Alexandra Myasnikova, Alexander Bogdanov, Viktorija Pankratova, Vladimir Pankratov, Ekaterina Kaneva, Roman Yu. Shendrik *

Posted Date: 13 May 2024

doi: 10.20944/preprints202405.0797.v1

Keywords: cesium iodide; ytterbium; luminescence; single crystal; Czochralski method

 doi:10.20944/preprints202405.0797.v1

Article

Crystal Growth and Spectroscopy of Yb^{2+} Doped CsI Single Crystal

Dmitriy Sofich [1,*], Alexandra Myasnikova [1], Alexander Bogdanov [1], Viktorija Pankratova [2], Vladimir Pankratov [2], Ekaterina Kaneva [1] and Roman Shendrik [1]

[1] Vinogradov Institute of Geochemistry, Irkutsk, Russia;
[2] Institute of Solid State Physics, University of Latvia, 8 Kengaraga Iela, LV-1063, Riga, Latvia
* Correspondence: sofich@igc.irk.ru;

Abstract: Solving the problem of searching for new scintillators based on available materials, we were the first to obtain and study a single crystal of CsI doped with divalent ytterbium ions. This work was directed to study of luminescence mechanism of Yb^{2+} ions and excitation transfer from crystalline matrix of CsI to dopant ions under VUV excitation. Using time-resolved spectroscopy, spin-allowed and spin-forbidden radiative transitions of ytterbium ions at room temperature were discovered. At 10 degrees, the emission of self-trapped excitons was detected. UV and VUV excitation spectra were obtained in the emission bands of ytterbium and self-trapped excitons. It was found that Yb^{2+} luminescence is excited in the excitonic region in the range of 10-45 eV. The mechanism of charge compensation of Yb^{2+} ions in a CsI crystal was also studied, the spectrum of the thermally stimulated depolarization current was measured, and the activation energies of the two observed peaks were calculated. These peaks belong to impurity-vacancy complexes in two different positions.It is concluded that Yb^{2+} ions are promising dopants for CsI scintillators and X-ray phosphors in combination with SiPM photodetectors.

Keywords: cesium iodide; ytterbium; luminescence; single crystal; Czochralski method

1. Introduction

Scintillators based on CsI have been known for quite a long time [1]. The most popular impurities for doping CsI crystals are Tl [2,3], Na [4,5] and Eu^{2+} [6–8]. Despite the fact that halide scintillators are emerging with greater efficiency than CsI, such as SrI_2-Eu [9–11], $LaBr_3$-Ce [12,13], BaBrI-Eu [14–16], BaBrCl-Eu [17], it does not lose its position on the market and remains one of the most popular scintillators at present. This is due to its relatively low price, as well as low hygroscopicity [18]. Currently, research is being conducted to increase the light output of CsI-Tl crystals using digital signal processing methods [19], modifying growth techniques [20], using photonic crystals [21], as well as co-doping with various cations [22]. Pure CsI crystals cooled to a temperature of 77 K exhibit high light output [23,24]. With increasing temperature, the decay of exciton excitations begins to occur non-radiatively, so CsI is doped with various impurities. The most studied process is the transfer of excitations to Tl^+ luminescence centers[3,25–27]. Promising impurities for halide scintillators are divalent lanthanides, in particular CsI-Eu^{2+}. However, the processes of energy transfer in these crystals have been studied in much less detail. However, effective energy transfer from self-trapped exciton to Eu^{2+} is noted[7].

Recently, other divalent lanthanides, such as Yb^{2+}, have begun to be used as activators for scintillation halide crystals [28–30] and Sm^{2+} [31–33]. Previously, the optical properties of Yb^{2+} in crystals with the NaCl structure were widely studied [34,35]. The work [36] notes that the intensity of X-ray luminescence increases under irradiation in NaCl-Yb^{2+} crystals. However, studies of CsI-Yb^{2+} crystals have not been previously carried out. Only some works [37,38] note that the addition of Yb to the charge when growing CsI-Tl crystals leads to a decrease in afterglow and an improvement in scintillation properties. However, confirmation that Yb^{2+} is present in the crystal structure was not obtained in these works; in particular, spectra were not given where absorption bands characteristic of the 4f-5d transitions would appear.

 doi:10.20944/preprints202405.0797.v1

In this work, a crystal study of crystal growth CsI-Yb^{2+} crystals and study 4f-5d transitions in Yb^{2+} using optical absorption, luminescence and thermally stimulated depolarization techniques is carried out. The prospects for doping CsI crystals with Yb^{2+} ions for use as scintillators are also being assessed.

2. Materials and Methods

CsI:Yb^{2+} single crystals were grown from the melt using the Czochralski method within a specialized single crystal growth facility. The growth unit consists of a spherical water-cooled chamber constructed from stainless steel. The crystal pulling rod is cooled by thermostatically controlled water and is operated by two stepper motors, enabling rotation and movement of the rod. At the end of the rod there is a graphite holder where a quartz capillary is installed. This setup is furnished with a thermal unit crafted from pyrolytic graphite; the heater takes on a cylindrical shape with vertical cuts, and a Type K thermocouple is affixed to the bottom of the crucible (Figure 1). To initiate the growth of a CsI:Yb^{2+} single crystal, 160 grams of crystalline ultradry CsI (Lanhit) with a purity of 99.998% (for metal impurities), along with 3 grams of YbI_2 with a purity of 99.99% (Lanhit), were utilized as initial components. Thus, the concentration of Yb in the melt was approximately 1 mol.%. The raw materials were loaded into a glassy carbon crucible and subjected to drying directly within the growth installation. The drying process entailed gradual heating and holding of the raw materials for five hours at a temperature of 500°C under vacuum. By the final stage of drying, the residual vapor pressure in the chamber was reduced to less than 0.01 Pa, indicating successful removal of absorbed impurities. Cesium iodide exhibits rapid evaporation in a vacuum; therefore, after drying, high-purity argon was introduced into the chamber until a pressure of 110 kPa was attained. Subsequently, the raw material was melted and overheated to 710°C for 1 hour to ensure homogenization. The temperature was then lowered to 645°C, corresponding to 625°C at the surface of the melt. The growth of a single crystal was facilitated by seeding onto a capillary, with the formation of a crystal neck.

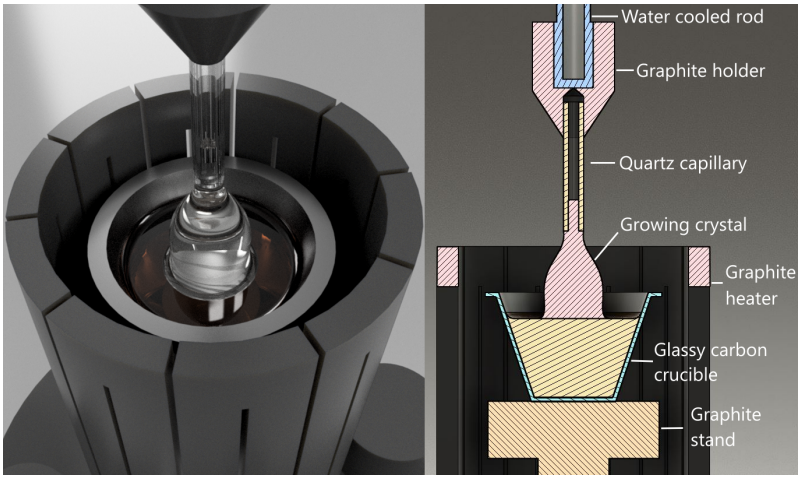

Figure 1. 3D model and schematic view of the equipment for crystal growth.

The CsI:Yb^{2+} crystal was grown at a rate of 1 mm per hour with a constant rotation of 1.2 revolutions per minute. The growth process lasted 42 hours, following which the crystal underwent annealing in a chamber for 30 hours, during which the temperature gradually decreased to eliminate internal stresses. The resulting single crystal measures 14 by 40 mm and exhibits no color; however, it displays intense blue luminescence when excited by a 395 nm UV diode (see Figure 2).

 doi:10.20944/preprints202405.0797.v1

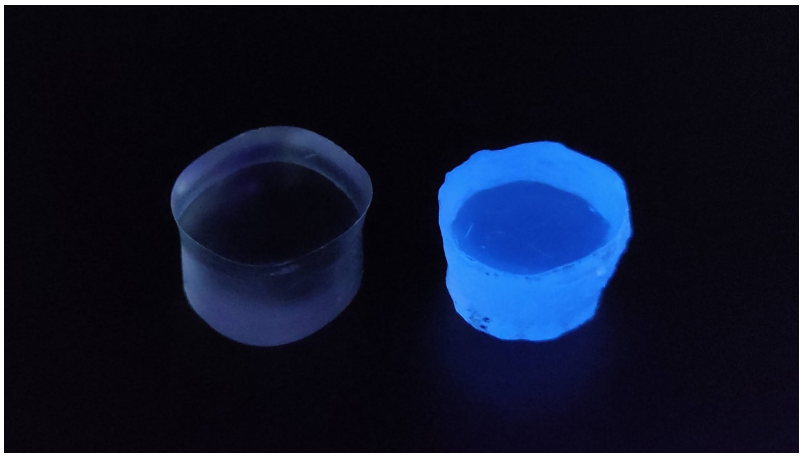

Figure 2. Luminescence of CsI:Yb^{2+} crystal (right) compared to a pure CsI crystal (left) under 395 nm excitation.

The samples have been cut in 2 and 10 mm thick plates and polished for optical experiments. Optical absorption spectra were measured using a Lambda 950 spectrophotometer (Perkin-Elmer, NY, USA). The luminescence time-resolved spectra were registered by an LS-55 spectrofluorimeter (Perkin-Elmer, NY, USA) and a spectrometer based on a SLD-1 and a MDR-2 grating monochromators (LOMO, Saint-Petersburg, Russia) equipped with the grating 1200 and 600 lines per mm. A photomultiplier module Hamamatsu H6780-04 was used as a photodetector. Ionic thermocurrent was measured using a picoampermeter A2-4 (MNIPI Minsk). Measurements were done in vacuum with Pt electrode and heating rate as 20 K min^{-1}. The sample (about 14 mm in diameter and about 1.6 mm thick) was attached to the cryostat with a spring-loaded platinum electrode, the polarization of the dipoles was carried out at room temperature with a voltage of 1.4 kV for 2–3 min, and then cooled to 90 K. Then the electrodes were connected to a picoammeter and the current was recorded during the heating process. The luminescence experiments under VUV excitations were carried out using synchrotron radiation from 1.5 GeV storage ring of MAX IV synchrotron facility (Lund, Sweden). The luminescence experiments under synchrotron radiation excitations are a powerful tool for the study of scintillators[39–41]. The experiments have been performed at the photoluminescence endstation of FinEstBeAMS beamline. The parameters of the beamline and the experimental setup are given in [42–46].

2.1. Theoretical Calculations

Geometry optimization for CsI-Yb^{2+} crystals was performed using density functional theory (DFT) within the VASP software package [47] and on the "Akademik V.M. Matrosov" computing cluster [48]. A 3x3x3 supercell with 216 atoms was constructed, with one Yb^{2+} ion replacing a lattice cation. Atomic positions and crystal symmetry were obtained from the ICSD database [49]. The PBEsol exchange-correlation functional and a G-centered grid of 8 k-points in the irreducible Brillouin zone were used for the gradient approximation geometry optimization, while preserving the cell shape and volume. Convergence was determined if the difference in total energies between iterations did not exceed 10^{-6}eV. The plane wave expansion energy cutoff was set as 500 eV.

Optical absorption spectra were calculated using the Orca software package [50]. A cluster consisting of a Yb^{2+} ion, 12 cesium ions, and 14 iodine ions was extracted from the optimized supercell. This quantum cluster was surrounded by several hundred cesium ions described by SDD pseudopotentials and several thousand point charges. The def2-TZVP pseudopotential was used for quantum domain calculations [51]. The TD-DFT (time dependent DFT) approach was employed for calculating optical transitions.

In the first step, the geometries of the lattice with a Yb^{2+} ion and a charge-compensating vacancy in the nearest or distant environment were calculated. In the case of a nearby vacancy, the absence of a cation resulted in significant displacements of ions surrounding the ytterbium ion. The maximum

 doi:10.20944/preprints202405.0797.v1

displacement of iodine ions was found to be 0.72 Å, which corresponds to 18% of the Cs-I distance in a defect-free crystal. The absence of one cation also led to a displacement of Cs ions, with a maximum displacement of 0.62 Å(15% of the Cs-I distance). Consequently, the defect caused a local reduction in symmetry. On the other hand, when the vacancy was situated far from the ytterbium ion (at the supercell boundary), the local environment retained octahedral symmetry. The maximum displacement of iodine ions towards the Yb^{2+} ion was 0.69 Å(17%), while the displacements of Cs ions were negligible.

3. Results

The CsI-Yb^{2+} crystal exhibits luminescence in the blue-green spectral range when excited at 3.4 and 4.55 eV. At 290 K, the luminescence is characterized by two bands centered at 2.6 and 2.8 eV (Figure 3, curve 2).

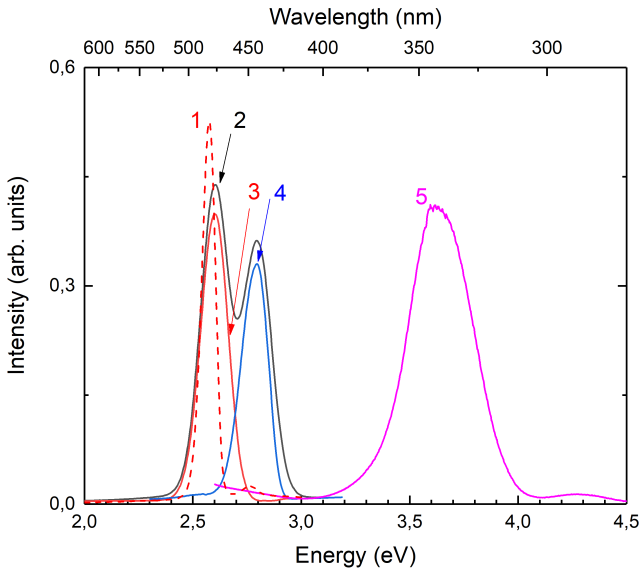

Figure 3. Luminescence spectra of the CsI-Yb^{2+} sample: (1) under 4.55 eV excitation at 10 K, (2) under 3.4 eV excitation at 290 K, (3) time-resolved luminescence in a long time window at 290 K un-der 3.4 eV excitation, (4) time-resolved luminescence in a short time window at 290 K under 3.4 eV excitation, (5) self-trapped exciton (STE) luminescence at 10 K under 5.9 eV excitation.

The higher energy band decays exponentially with a time constant of approximately 120 ns (Figure 3, curve 3), while the lower energy band at 2.6 eV also decays exponentially with a time constant of 325 μs (Figure 3, curve 4). As the crystal cools, the intensity of the higher energy band at 2.8 eV decreases, while the intensity of the 2.6 eV band increases and slightly shifts to a lower energy region (Figure 3, curve 1). At lower temperatures, a new luminescence band centered at 3.6 eV appears under excitation at 5.9 eV (Figure 3, curve 5).

The absorption spectrum of CsI-Yb^{2+} reveals four bands at 3.05, 3.4, 3.9, and 4.55 eV (Figure 4 a, dashed curve). The excitation spectrum, measured at 2.6 and 2.8 eV, shows six bands at 3.05, 3.4, 3.9, 4.55, 5.2, and 5.6 eV. Additionally, there are weak, sharper structured bands observed near 5.9 eV (Figure 4 a, black curve).

The excitation spectrum of the self-trapped exciton luminescence is presented in Figure 4 (a, blue curve). It shows a peak at 5.9 eV and a sharp dip structure in the range between 5.75 eV and 6.3 eV. The dips in the spectrum are located at 5.83, 5.93, 6.00, and 6.25 eV (Figure 4, b).

 doi:10.20944/preprints202405.0797.v1

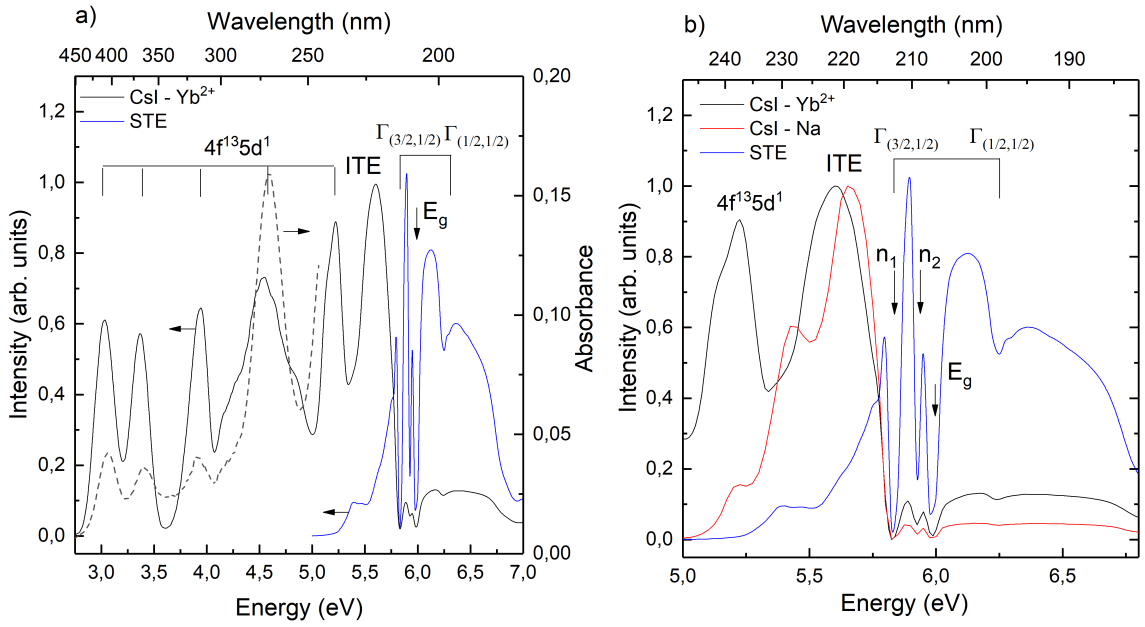

Figure 4. The absorption spectrum (dashed curve 1) and excitation spectra of CsI-Yb^{2+} monitored at 2.6 eV (black curve) and at 3.6 eV (blue curve) (a). The subfigure (b) presents an enlarged region of band-to-band transitions.

The comparison of experimental and calculated absorption spectra is given in Figure 5. The black vertical lines show the $4f^{14}$-$4f^{13}5d^1$ transitions in the Yb^{2+} ion compensated by the cation vacancy in the next-nearest-neighbor position (nnn), while the red vertical lines show the $4f^{14}$-$4f^{13}5d^1$ transitions in the Yb^{2+} ion when the cation vacancy is located in the nearest-neighbor (nn) position.

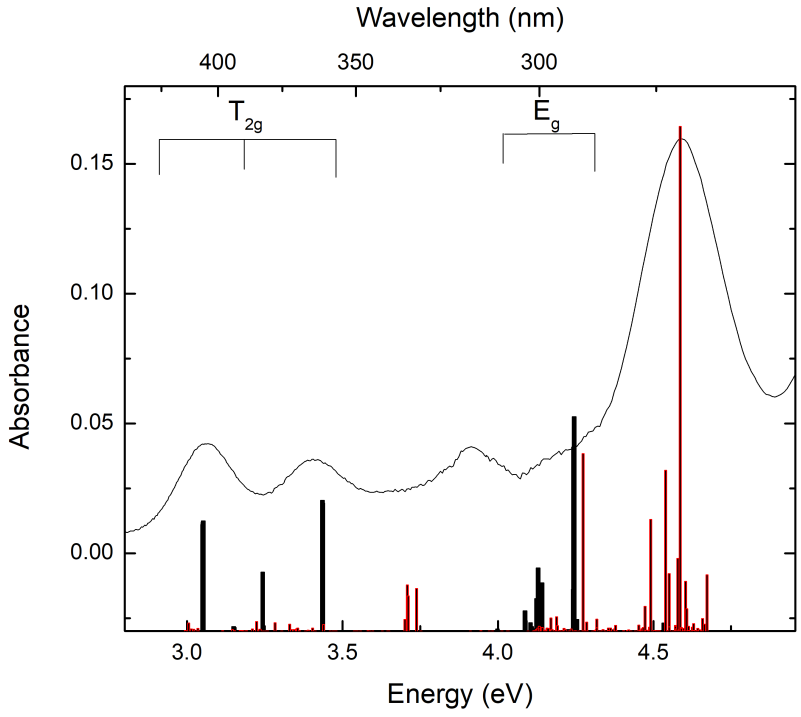

Figure 5. The absorption spectrum (solid curve) and calculated positions of $4f^{14}$-$4f^{13}5d^1$ transitions in the Yb^{2+} ion with a cation vacancy in the nearest neighbor (red lines) and the next-nearest neighbor (black lines) positions.

 doi:10.20944/preprints202405.0797.v1

The excitation spectra, monitored at 2.6 eV and 3.6 eV, in the higher energy range of 7-45 eV are depicted in Figure 6. It is evident from the spectra that there is an increase in intensity at energies exceeding 12 eV.

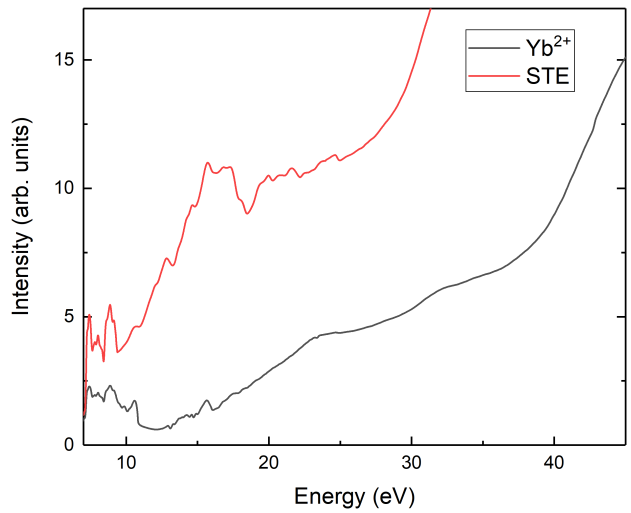

Figure 6. Excitation spectra monitored at 2.6 eV (black curve) and at 3.6 eV (red curve) in the energy region of 7-45 eV.

The polarized CsI crystals doped with Yb^{2+} ions, cooled to 80 K, display prominent peaks in the thermally stimulated depolarization current at 190 and 205 K (Figure 7), in contrast to nominally pure CsI. The intensity of these peaks is observed to rise with an increase in the concentration of Yb^{2+} ions.

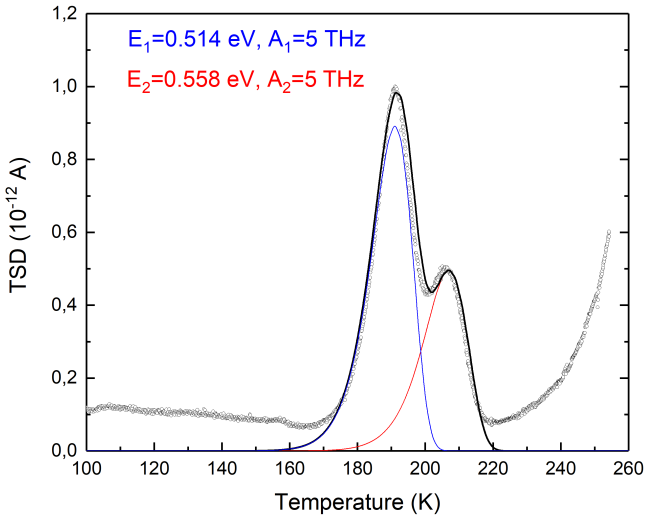

Figure 7. Thermally stimulated depolarization current curve of CsI-Yb^{2+}.

4. Discussion

Due to the closed 4f shell in Yb^{2+} doped materials, only broad luminescence bands attributed to transitions from the excited $4f^{13}$-$5d^1$ state to the ground $4f^{14}$ state are observed. Generally, the 5d-4f emission of Yb^{2+} ions exhibits two bands due to the half-filled 4f shell. These bands correspond to a

 doi:10.20944/preprints202405.0797.v1

spin-forbidden high-spin transition, where excitation occurs with a reversal of spin, and a spin-allowed low-spin transition. The high-spin excited states have lower energy than the low-spin transitions, following Hund's rules. Therefore, the observed luminescence band at 2.6 eV corresponds to the high-spin 5d-4f transition in Yb^{2+} ions, while the higher energy band at 2.8 eV is attributed to the low-spin 5d-4f transition. Yb^{2+} doped alkali halides and alkali earth halides have been extensively studied [52]. Both spin-forbidden and spin-allowed emissions are observed in NaCl-Yb^{2+} and SrI_2:Yb^{2+}[34]. The kinetic of luminescence was calculated for NaCl-Yb in [53].

Optical absorption spectra associated with Yb^{2+} in KI, NaI, KBr, NaBr, KCl, NaCl, and KF were obtained at both room and liquid nitrogen temperatures. In NaCl [34] and KCl, NaBr [54], nine groups of lines attributed to $4f^{14}$-$4f^{13}5d^1$ transitions were identified. The excited $4f^{13}5d^1$ configuration of Yb^{2+} decomposes into a total of 58 levels under an octahedral crystal field, with 20 free-ion levels associated with it [55]. The theoretical analysis of the absorption spectra for the Oh point group was performed in [34], while an increase in absorption bands was observed for the C_{2v} point group in the case of cation vacancy charge compensation [56]. The position of absorption bands was found to strongly depend on the strength of the crystal-field parameter B in different types of charge compensation scenarios. The ab initio calculation without spin-orbital coupling predicts 4 groups of levels corresponding to $4f^{13}(^2F_{7/2})5d^1$(t2g). However, the inclusion of spin-orbital coupling leads to the appearance of a higher energy transition attributed to $4f^{13}(^2F_{5/2})5d^1$(t2g).

The ab initio calculation shows that the lowest energy bands in the absorption spectra correspond to transitions to triple degenerated 5d T_{2g} states, but higher energy transitions are attributed to transitions to double degenerated E_g states (Figure 5) in the nnn configuration when the cation vacancy is located in the next-nearest neighbor position. The position of the 4f-5d absorption bands for the divalent Yb ion compensated by a cation vacancy in the nearest neighbor configuration has higher energy and larger intensity. The observed absorption spectrum contains the contributions from both Yb^{2+} centers.

The Yb^{2+} ions replace Cs^+ ions in the material, necessitating charge compensation. This compensation can occur through the presence of interstitial iodine ions or cation vacancies in nearest-neighbor (nn) and next nearest-neighbor (nnn) positions. The experimental absorption and excitation spectra are in good agreement with the calculated Yb^{2+} centers compensated by cation vacancies in the nn and nnn configuration. The Yb^{2+}-iodine vacancy and Yb^{2+}-cation vacancy combinations form electrical dipoles. As a result, they can be polarized at low temperatures and subsequently depolarized during heating. This phenomenon gives rise to a thermally stimulated depolarization (TSD) curve. The TSD curve exhibits two closely located peaks at 195 and 205 K, which can be well described by a first-order kinetic equation for thermally stimulated processes [57](Eq. 1).

$$I_{TL} = n_0 s \exp\left\{-\frac{E_t}{kT}\right\} \exp\left\{-\left(\frac{s}{\beta}\right)\int_{T_0}^{T} \exp\left\{-\frac{E_t}{k\theta}\right\} d\theta\right\}, \quad (1)$$

The activation energies are 0.514 eV and 0.558 eV. The frequency factor, s = 5 THz, corresponds to the phonon modes present in CsI. The observed peaks are attributed to Yb^{2+}-cation vacancy dipoles, also known as I-V complexes. The lower energy peak is related to the reorientation of nearest-neighbor (nn) dipoles, while the peaks at 205 K correspond to the reorientation of next nearest-neighbor (nnn) dipoles.

Similar thermally stimulated depolarization (TSD) phenomena have been observed in NaCl-type crystals doped with divalent cations within the temperature range of 190-230 K. The observed peaks in these crystals are also attributed to I-V complexes [58,59] in nn and nnn positions. In NaCl, the nn peak is located at 210 K, while the nnn peak is located at 230 K.

The presence of I-V centers in the TSD curve confirms that the charge compensation for Yb^{2+} occurs through cation vacancies. The intensity of TSD peaks attributed to I-V complexes in nn coordination is higher, indicating that the charge compensation mainly occurs through nearest-neighbor cation vacancies. The luminescence band at 3.6 eV is excited at approximately 5.8-6.0 eV and exhibits

 doi:10.20944/preprints202405.0797.v1

a sharp structure. The dips at 5.83, 5.93, 6.00, and 6.25 eV correspond to the n1 and n2 levels of the Γ (3/2, 1/2) exciton [33,60]. The observed structure is consistent with theoretical calculations and the experimental absorption spectrum of thin films of CsI [61]. The luminescence band at 3.6 eV corresponds to luminescence from off-center self-trapped excitons (STE) in CsI [62]. This band coincides with the wavelength range of the 4f-5d absorption of Yb^{2+} ions, indicating the possibility of exciton energy transfer to Yb^{2+} ions. This is supported by the presence of similar bands in the excitation spectrum of Yb^{2+} within the exciton excitation region. Similar energy transfer mechanisms have been observed in other effective halide scintillators such as CsI-Tl [63] and CsI-Eu [3], BaBrI-Eu [16], BaBrI-Ce [64], BaBrCl-Eu [65]. The excitation spectrum in the vacuum ultraviolet (VUV) region demonstrates the multiplication of electronic excitations. Although not as pronounced as in STE, increasing the concentration of Yb^{2+} up to 0.3-1 mol.% is expected to enhance the multiplications due to an increase in exciton energy transfer deposition.

The Yb^{2+} luminescence region coincides with the peak sensitivity of SiPM (Silicon Photomultiplier) detectors. Therefore, Yb^{2+} ions are promising dopants for CsI scintillators and X-ray phosphors when combined with SiPM photodetectors.

5. Conclusions

The first time CsI doped Yb^{2+} single crystal was given. The charge compensation of Yb^{2+} occurs in the nearest neighbor and next nearest neighbor cation vacancies. The luminescence attributed to 5d-4f spin-allowed and spin-forbidden transitions was observed at 300 K. In the cooled-down samples, only spin-forbidden luminescence was detected. The excitation and absorption spectra of CsI-Yb^{2+} crystals demonstrate strong bands attributed to the 4f-5d transition in the energy range between 2.7-5.7 eV. The luminescence of Yb^{2+} is also excited in the excitonic range and demonstrates multiplication of electronic excitation in the range 10-45 eV. That allows us to expect the promising scintillation properties of Yb^{2+} in CsI.

Funding: This work (crystal growth, spectroscopy and measurements of dielectric properties) was funded by the Russian Science Foundation (project No. 23-72-01097).

Acknowledgments: The geometry optimization was supported by Russian academy of Science basic program. The work of Vladimir Pankratov is supported by the LZP grant (2022/1-0611), while Viktorija Pankratova acknowledges the LZP grant (2023/1-0453). The Institute of Solid State Physics, University of Latvia as the Center of Excellence has received funding from the European Union's Horizon 2020 Framework Programme H2020-WIDESPREAD-01-2016-2017-TeamingPhase2 under grant agreement No. 739508, project CAMART2. We acknowledge MAX IV Laboratory for time on FinEstBeAMS Beamline under Proposal 20211074. Research conducted at MAX IV, a Swedish national user facility, is supported by the Swedish Research council under contract 2018-07152, the Swedish Governmental Agency for Innovation Systems under contract 2018-04969, and Formas under contract 2019-02496. The authors are grateful to Kirill Chernenko for help with measurements at the MAX IV synchrotron facility.

Conflicts of Interest: The authors declare no conflicts of interest.

Abbreviations

The following abbreviations are used in this manuscript:

VUV	Vacuum ultraviolet
VASP	The Vienna Ab initio Simulation Package
SiPM	Silicon photomultiplier
STE	Self-trapped exciton

References

1. Van Sciver, W.; Hofstadter, R. Scintillations in Thallium-Activated CaI_2 and CsI. *Physical Review* **1951**, *84*, 1062–1063. Publisher: American Physical Society, doi:10.1103/PhysRev.84.1062.2.

2. Aitken, D.W.; Beron, B.L.; Yenicay, G.; Zulliger, H.R. The Fluorescent Response of NaI(Tl), CsI(Tl), CsI(Na) and CaF_2(Eu) to X-Rays and Low Energy Gamma Rays. *IEEE Transactions on Nuclear Science* **1967**, *14*, 468–477. Conference Name: IEEE Transactions on Nuclear Science, doi:10.1109/TNS.1967.4324457.
3. Yakovlev, V.; Trefilova, L.; Meleshko, A.; Alekseev, V.; Kosinov, N. Charge transfer processes in CsI:Tl using near-UV light. *Journal of Luminescence* **2014**, *155*, 79–83. doi:10.1016/j.jlumin.2014.05.019.
4. Imanaka, K.; Kayal, A.H.; Mezger, A.C.; Rossel, J. Self-Trapped Exciton Luminescence after Tunnelling of Vk and Nao Centers in CsI:Na Crystals. *physica status solidi (b)* **1981**, *108*, 449–458. doi:10.1002/pssb.2221080220.
5. Yakovlev, V.; Trefilova, L.; Meleshko, A.; Ganja, Y. Short-living absorption and emission of CsI(Na). *Journal of Luminescence* **2011**, *131*, 2579–2581. doi:10.1016/j.jlumin.2011.06.037.
6. Savel'ev, V.; Avdonin, V.; Dugarova, L.; Nedashkovskij, A.; Plachenov, B. Aggregation of Eu^{2+}centers in alkali halide crystals doped with Eu. *Fizika Tverdogo Tela* **1974**, *16*, 1090–1093. Place: USSR INIS Reference Number: 5140083.
7. Yakovlev, V.; Trefilova, L.; Karnaukhova, A.; Ovcharenko, N. Energy transfer mechanism in CsI:Eu crystal. *Journal of Luminescence* **2014**, *148*, 274–276. doi:10.1016/j.jlumin.2013.12.020.
8. Gektin, A.; Shiran, N.; Belsky, A.; Vasyukov, S. Luminescence properties of CsI:Eu crystals. *Optical Materials* **2012**, *34*, 2017–2020. doi:10.1016/j.optmat.2012.02.010.
9. Shoji, Y.; Kurosawa, S.; Yokota, Y.; Hayasaka, S.; Kamada, K.; Yoshino, M.; Yamaji, A.; Chani, V.; Ohashi, Y.; Sakuragi, S.; Yoshikawa, A. Growth and Scintillation Properties of Two-Inch-Diameter SrI_2(Eu) Single Crystals. *Crystal Growth & Design* **2018**, *18*, 3747–3752. Publisher: American Chemical Society, doi:10.1021/acs.cgd.7b01044.
10. Galenin, E.; Sidletskiy, O.; Dujardin, C.; Gektin, A. Growth and Characterization of SrI_2:Eu Crystals Fabricated by the Czochralski Method. *IEEE Transactions on Nuclear Science* **2018**, *65*, 2174–2177. Conference Name: IEEE Transactions on Nuclear Science, doi:10.1109/TNS.2017.2787420.
11. Smerechuk, A.; Galenin, E.; Nesterkina, V.; Sidletskiy, O.; Dujardin, C. Growth and scintillation performances of SrI_2:Eu with low activator concentration. *Journal of Crystal Growth* **2019**, *521*, 41–45. doi:10.1016/j.jcrysgro.2019.05.031.
12. van Loef, E.V.D.; Dorenbos, P.; van Eijk, C.W.E.; Krämer, K.; Güdel, H.U. High-energy-resolution scintillator: Ce^{3+} activated $LaBr_3$. *Applied Physics Letters* **2001**, *79*, 1573–1575. doi:10.1063/1.1385342.
13. Alekhin, M.S.; de Haas, J.T.M.; Khodyuk, I.V.; Krämer, K.W.; Menge, P.R.; Ouspenski, V.; Dorenbos, P. Improvement of γ-ray energy resolution of $LaBr_3$:Ce3+ scintillation detectors by Sr^{2+} and Ca^{2+} co-doping. *Applied Physics Letters* **2013**, *102*, 161915. doi:10.1063/1.4803440.
14. Bourret-Courchesne, E.D.; Bizarri, G.; Hanrahan, S.M.; Gundiah, G.; Yan, Z.; Derenzo, S.E. BaBrI:Eu^{2+}, a new bright scintillator. *Nuclear Instruments and Methods in Physics Research Section A: Accelerators, Spectrometers, Detectors and Associated Equipment* **2010**, *613*, 95–97. doi:10.1016/j.nima.2009.11.036.
15. Shendrik, R.; Shalaev, A.A.; Myasnikova, A.S.; Bogdanov, A.; Kaneva, E.; Rusakov, A.; Vasilkovskyi, A. Optical and structural properties of Eu^{2+} doped BaBrI and BaClI crystals. *Journal of Luminescence* **2017**, *192*, 653–660. doi:10.1016/j.jlumin.2017.07.059.
16. Shalaev, A.A.; Shendrik, R.; Myasnikova, A.S.; Bogdanov, A.; Rusakov, A.; Vasilkovskyi, A. Luminescence of BaBrI and SrBrI single crystals doped with Eu^{2+}. *Optical Materials* **2018**, *79*, 84–89. https://doi.org/10.1016/j.optmat.2018.03.017.
17. Shalapska, T.; Moretti, F.; Bourret, E.; Bizarri, G. Effect of Au codoping on the scintillation properties of BaBrCl:Eu single crystals. *Journal of Luminescence* **2018**, *202*, 497–501. doi:10.1016/j.jlumin.2018.06.019.
18. Zhuravleva, M.; Stand, L.; Wei, H.; Hobbs, C.; Boatner, L.A.; Ramey, J.O.; Shah, K.; Burger, A.; Rowe, E.; Bhattacharya, P.; Tupitsyn, E.; Melcher, C.L. Hygroscopicity evaluation of halide scintillators. 2013 IEEE Nuclear Science Symposium and Medical Imaging Conference (2013 NSS/MIC), 2013, pp. 1–5. ISSN: 1082-3654, doi:10.1109/NSSMIC.2013.6829669.
19. Mianowska, Z.; Moszynski, M.; Brylew, K.; Chabera, M.; Dziedzic, A.; Gektin, A.V.; Krakowski, T.; Mianowski, S.; Syntfeld-Każuch, A.; Szczesniak, T.; Zezulinski, K. The light response of CsI:Tl crystal after interaction with gamma radiation study using analysis of single scintillation pulses and digital oscilloscope readout. *Nuclear Instruments and Methods in Physics Research Section A: Accelerators, Spectrometers, Detectors and Associated Equipment* **2022**, *1031*, 166600. doi:10.1016/j.nima.2022.166600.

 doi:10.20944/preprints202405.0797.v1

20. Wang, W.; Qi, H.; Liu, F.; Meng, H.; Cai, J.; Xu, S.; Jing, S.; Hong, F.; Zhu, Y.; Xu, H.; Xu, R.; Lai, J.; Xu, F.; Wang, L. Approaching the Theoretical Light Yield Limit in CsI (Tl) Scintillator Single Crystals by a Low-Temperature Solution Method. *Crystal Growth & Design* **2020**, *20*, 3474–3481. Publisher: American Chemical Society, doi:10.1021/acs.cgd.0c00256.
21. Ouyang, X.; Liu, B.; Xiang, X.; Chen, L.; Xu, M.; Song, X.; Ruan, J.; Liu, J.; Chen, C.; Zhu, Z.; Li, Y. Enhanced light output of CsI(Na) scintillators by photonic crystals. *Nuclear Instruments and Methods in Physics Research Section A: Accelerators, Spectrometers, Detectors and Associated Equipment* **2020**, *969*, 164007. doi:10.1016/j.nima.2020.164007.
22. Sisodiya, D.S.; Singh, S.G.; Chandrakumar, K.R.S.; Patra, G.D.; Ghosh, M.; Pitale, S.; Sen, S. Optimizing the Scintillation Kinetics of CsI Scintillator Single Crystals by Divalent Cation Doping: Insights from Electronic Structure Analysis and Luminescence Studies. *The Journal of Physical Chemistry C* **2024**, *128*, 197–209. Publisher: American Chemical Society, doi:10.1021/acs.jpcc.3c06098.
23. Ding, K.; Chernyak, D.; Liu, J. Light yield of cold undoped CsI crystal down to 13 keV and the application of such crystals in neutrino detection. *The European Physical Journal C* **2020**, *80*, 1146. doi:10.1140/epjc/s10052-020-08712-2.
24. Mikhailik, V.B.; Kapustyanyk, V.; Tsybulskyi, V.; Rudyk, V.; Kraus, H. Luminescence and scintillation properties of CsI: A potential cryogenic scintillator. *physica status solidi (b)* **2015**, *252*, 804–810. doi:10.1002/pssb.201451464.
25. Popov, A.I.; Chernov, S.A.; Trinkler, L.E. Time-resolved luminescence of CsI:Tl crystals excited by pulsed electron beam. *Nuclear Instruments and Methods in Physics Research Section B: Beam Interactions with Materials and Atoms* **1997**, *122*, 602–605. doi:10.1016/S0168-583X(96)00664-7.
26. Williams, R.T.; Grim, J.Q.; Li, Q.; Ucer, K.B.; Moses, W.W. Excitation density, diffusion-drift, and proportionality in scintillators. *physica status solidi (b)* **2011**, *248*, 426–438. doi:10.1002/pssb.201000610.
27. Hamada, M.M.; Costa, F.E.; Shimizu, S.; Kubota, S. Radiation damage of CsI(Tl) scintillators: blocking of energy transfer process of V_k centers to Tl^+ activators. *Nuclear Instruments and Methods in Physics Research Section A: Accelerators, Spectrometers, Detectors and Associated Equipment* **2002**, *486*, 330–335. doi:10.1016/S0168-9002(02)00729-5.
28. Suta, M.; Wickleder, C. Spin Crossover of Yb^{2+} in $CsCaX_2$ and $CsSrX_2$ (X = Cl, Br, I) – A Guideline to Novel Halide-Based Scintillators. *Advanced Functional Materials* **2017**, *27*, 1602783. doi:10.1002/adfm.201602783.
29. Suta, M.; Wickleder, C. Synthesis, spectroscopic properties and applications of divalent lanthanides apart from Eu^{2+}. *Journal of Luminescence* **2019**, *210*, 210–238. doi:10.1016/j.jlumin.2019.02.031.
30. Mizoi, K.; Arai, M.; Fujimoto, Y.; Nakauchi, D.; Koshimizu, M.; Yanagida, T.; Asai, K. Photoluminescence and scintillation properties of Yb^{2+}-doped $ACaCl_3$ (A = Cs, Rb, K) crystals. *Journal of Luminescence* **2020**, *227*, 117521. doi:10.1016/j.jlumin.2020.117521.
31. Wolszczak, W.; Krämer, K.W.; Dorenbos, P. Engineering near-infrared emitting scintillators with efficient $Eu^{2+} \rightarrow Sm^{2+}$ energy transfer. *Journal of Luminescence* **2020**, *222*, 117101. doi:10.1016/j.jlumin.2020.117101.
32. Shalaev, A.A.; Shendrik, R.Y.; Rusakov, A.I.; Sokol'nikova, Y.V.; Myasnikova, A.S. Growth and Study of Scintillation Properties of BaBrI Crystals Activated by Samarium Ions. *Physics of the Solid State* **2019**, *61*, 2403–2406. doi:10.1134/S1063783419120497.
33. Shalaev, A.; Shendrik, R.; Rusakov, A.; Bogdanov, A.; Pankratov, V.; Chernenko, K.; Myasnikova, A. Luminescence of divalent lanthanide doped BaBrI single crystal under synchrotron radiation excitations. *Nuclear Instruments and Methods in Physics Research Section B: Beam Interactions with Materials and Atoms* **2020**, *467*, 17–20. doi:10.1016/j.nimb.2020.01.023.
34. Tsuboi, T.; Witzke, H.; McClure, D.S. The $4f^{14} \rightarrow 4f^{13}5d$ transition of Yb^{2+} ion in NaCl crystals. *Journal of Luminescence* **1981**, *24-25*, 305–308. doi:10.1016/0022-2313(81)90278-7.
35. O., J.R. Doubly-valent rare-earth ions in halide crystals. *Journal of Physics and Chemistry of Solids* **1991**, *52*, 101–174. doi:10.1016/0022-3697(91)90062-5.
36. Fujimoto, Y.; Okada, G.; Sekine, D.; Yanagida, T.; Koshimizu, M.; Kawamoto, H.; Asai, K. Radiation induced change in the optical properties of NaCl:Yb crystal. *Radiation Measurements* **2020**, *133*, 106274. doi:10.1016/j.radmeas.2020.106274.
37. Wu, Y.; Ren, G.; Nikl, M.; Chen, X.; Ding, D.; Li, H.; Pan, S.; Yang, F. CsI:Tl+,Yb^{2+}: ultra-high light yield scintillator with reduced afterglow. *CrystEngComm* **2014**, *16*, 3312–3317. Publisher: The Royal Society of Chemistry, doi:10.1039/C3CE42645A.

38. Bartram, R.H.; Kappers, L.A.; Hamilton, D.S.; Brecher, C.; Ovechkina, E.E.; Miller, S.R.; Nagarkar, V.V. Multiple thermoluminescence glow peaks and afterglow suppression in CsI:Tl co-doped with Eu^{2+} or Yb^{2+}. *IOP Conference Series: Materials Science and Engineering* **2015**, *80*, 012003. Publisher: IOP Publishing, doi:10.1088/1757-899X/80/1/012003.
39. Pankratova, V.; Kozlova, A.P.; Buzanov, O.A.; Chernenko, K.; Shendrik, R.; Šarakovskis, A.; Pankratov, V. Time-resolved luminescence and excitation spectroscopy of co-doped $Gd_3Ga_3Al_2O_{12}$ scintillating crystals. *Scientific Reports* **2020**, *10*, 20388. Publisher: Nature Publishing Group, doi:10.1038/s41598-020-77451-x.
40. Tuomela, A.; Zhang, M.; Huttula, M.; Sakirzanovas, S.; Kareiva, A.; Popov, A.I.; Kozlova, A.P.; Aravindh, S.A.; Cao, W.; Pankratov, V. Luminescence and vacuum ultraviolet excitation spectroscopy of samarium doped SrB_4O_7. *Journal of Alloys and Compounds* **2020**, *826*, 154205. doi:10.1016/j.jallcom.2020.154205.
41. Kozlova, A.P.; Kasimova, V.M.; Buzanov, O.A.; Chernenko, K.; Klementiev, K.; Pankratov, V. Luminescence and vacuum ultraviolet excitation spectroscopy of cerium doped $Gd_3Ga_3Al_2O_{12}$ single crystalline scintillators under synchrotron radiation excitations. *Results in Physics* **2020**, *16*, 103002. doi:10.1016/j.rinp.2020.103002.
42. Chernenko, K.; Kivimäki, A.; Pärna, R.; Wang, W.; Sankari, R.; Leandersson, M.; Tarawneh, H.; Pankratov, V.; Kook, M.; Kukk, E.; Reisberg, L.; Urpelainen, S.; Käämbre, T.; Siewert, F.; Gwalt, G.; Sokolov, A.; Lemke, S.; Alimov, S.; Knedel, J.; Kutz, O.; Seliger, T.; Valden, M.; Hirsimäki, M.; Kirm, M.; Huttula, M. Performance and characterization of the FinEstBeAMS beamline at the MAX IV Laboratory. *Journal of Synchrotron Radiation* **2021**, *28*, 1620–1630. Publisher: International Union of Crystallography, doi:10.1107/S1600577521006032.
43. Pärna, R.; Sankari, R.; Kukk, E.; Nõmmiste, E.; Valden, M.; Lastusaari, M.; Kooser, K.; Kokko, K.; Hirsimäki, M.; Urpelainen, S.; Turunen, P.; Kivimäki, A.; Pankratov, V.; Reisberg, L.; Hennies, F.; Tarawneh, H.; Nyholm, R.; Huttula, M. FinEstBeaMS – A wide-range Finnish-Estonian Beamline for Materials Science at the 1.5 GeV storage ring at the MAX IV Laboratory. *Nuclear Instruments and Methods in Physics Research Section A: Accelerators, Spectrometers, Detectors and Associated Equipment* **2017**, *859*, 83–89. doi:10.1016/j.nima.2017.04.002.
44. Pankratov, V.; Kotlov, A. Luminescence spectroscopy under synchrotron radiation: From *SUPERLUMI* to *FINESTLUMI*. *Nuclear Instruments and Methods in Physics Research Section B: Beam Interactions with Materials and Atoms* **2020**, *474*, 35–40. doi:10.1016/j.nimb.2020.04.015.
45. Pankratov, V.; Pärna, R.; Kirm, M.; Nagirnyi, V.; Nõmmiste, E.; Omelkov, S.; Vielhauer, S.; Chernenko, K.; Reisberg, L.; Turunen, P.; Kivimäki, A.; Kukk, E.; Valden, M.; Huttula, M. Progress in development of a new luminescence setup at the *FinEstBeAMS* beamline of the MAX IV laboratory. *Radiation Measurements* **2019**, *121*, 91–98. doi:10.1016/j.radmeas.2018.12.011.
46. Shendrik, R.; Kaneva, E.; Pankratova, V.; Pankrushina, E.; Radomskaya, T.; Gavrilenko, V.; Loginova, P.; Pankratov, V. Intrinsic luminescence and radiation defects in scapolite. *Chemical Physics Letters* **2024**, *838*, 141081. doi:10.1016/j.cplett.2024.141081.
47. Kresse, G.; Hafner, J. Ab initiomolecular dynamics for liquid metals. *Physical Review B* **1993**, *47*, 558–561. doi:10.1103/physrevb.47.558.
48. HPC-cluster "Akademik V.M. Matrosov". Irkutsk Supercomputer Center of SB RAS.
49. Inorganic Crystal Structure Database. FIZ Karlsruhe – Leibniz Institute for Information Infrastructure.
50. Neese, F. The ORCA program system. *WIREs Computational Molecular Science* **2011**, *2*, 73–78. https://doi.org/10.1002/wcms.81.
51. Pritchard, B.P.; Altarawy, D.; Didier, B.; Gibson, T.D.; Windus, T.L. New Basis Set Exchange: An Open, Up-to-Date Resource for the Molecular Sciences Community. *Journal of Chemical Information and Modeling* **2019**, *59*, 4814–4820. doi:10.1021/acs.jcim.9b00725.
52. Suta, M.; Urland, W.; Daul, C.; Wickleder, C. Photoluminescence properties of Yb^{2+} ions doped in the perovskites $CsCaX_3$ and $CsSrX_3$ (X = Cl, Br, and I) – a comparative study. *Physical Chemistry Chemical Physics* **2016**, *18*, 13196–13208. Publisher: The Royal Society of Chemistry, doi:10.1039/C6CP00085A.
53. Tsuboi, T.; McClure, D.S.; Wong, W.C. Luminescence kinetics of Yb^{2+} in NaCl. *Physical Review B* **1993**, *48*, 62–67. Publisher: American Physical Society, doi:10.1103/PhysRevB.48.62.
54. Bland, S.W.; Smith, M.J.A. $4f^{14}$ to $4f^{13}5d$ optical transitions of divalent ytterbium in the potassium and sodium halides. *Journal of Physics C: Solid State Physics* **1985**, *18*, 1525. doi:10.1088/0022-3719/18/7/018.

55. Bryant, B.W. Spectra of Doubly and Triply Ionized Ytterbium, Yb III and Yb IV. *JOSA* **1965**, *55*, 771–779. Publisher: Optica Publishing Group, doi:10.1364/JOSA.55.000771.
56. Duan, C.K.; Tanner, P.A. Simulation of 4f–5d transitions of Yb^{2+} in potassium and sodium halides. *Journal of Physics: Condensed Matter* **2008**, *20*, 215228. doi:10.1088/0953-8984/20/21/215228.
57. Randall, J.T.; Wilkins, M.H.F.; Oliphant, M.L.E. Phosphorescence and electron traps - I. The study of trap distributions. *Proceedings of the Royal Society of London. Series A. Mathematical and Physical Sciences* **1997**, *184*, 365–389. Publisher: Royal Society, doi:10.1098/rspa.1945.0024.
58. Capelletti, R. Thermally Stimulated Depolarization Studies of Ionic Solids. In *Defects in Solids: Modern Techniques*; Chadwick, A.V.; Terenzi, M., Eds.; Springer US: Boston, MA, 1986; pp. 407–431. doi:10.1007/978-1-4757-0761-8_19.
59. Poźniak, J.; Poźniak, J.K. Thermally Stimulated Depolarization Currents in Me^{2+}-Doped NaCl-Type Alkali Halide Crystals. *physica status solidi (b)* **1997**, *200*, 535–544. doi:10.1002/1521-3951(199704)200:2<535::AID-PSSB535>3.0.CO;2-U.
60. Matsumoto, T.; Shirai, M.; Kan'no, K.i. Time-Resolved Spectroscopic Study on the Type I Self-Trapped Excitons in Alkali Halide Crystals: II. Excitation Spectra and Relaxation Processes. *Journal of the Physical Society of Japan* **1995**, *64*, 987–1001. Publisher: The Physical Society of Japan, doi:10.1143/JPSJ.64.987.
61. Onodera, Y. Energy Bands in CsI. *Journal of the Physical Society of Japan* **1968**, *25*, 469–480. Publisher: The Physical Society of Japan, doi:10.1143/JPSJ.25.469.
62. Lu, X.; Li, Q.; Bizarri, G.A.; Yang, K.; Mayhugh, M.R.; Menge, P.R.; Williams, R.T. Coupled rate and transport equations modeling proportionality of light yield in high-energy electron tracks: CsI at 295 K and 100 K; CsI:Tl at 295 K. *Physical Review B* **2015**, *92*, 115207. Publisher: American Physical Society, doi:10.1103/PhysRevB.92.115207.
63. Williams, R.T.; Ucer, K.B.; Grim, J.Q.; Lipke, K.C.; Trefilova, L.M.; Moses, W.W. Picosecond Studies of Transient Absorption Induced by BandGap Excitation of CsI and CsI:Tl at Room Temperature. *IEEE Transactions on Nuclear Science* **2010**, *57*, 1187–1192. Conference Name: IEEE Transactions on Nuclear Science, doi:10.1109/TNS.2009.2033184.
64. Shendrik, R.Y.; Kovalev, I.I.; Rusakov, A.I.; Sokol'nikova, Y.V.; Shalaev, A.A. Luminescence of BaBrI Crystals Doped with Ce^{3+} Ions. *Physics of the Solid State* **2019**, *61*, 830–834. doi:10.1134/S1063783419050329.
65. Li, P.; Gridin, S.; Ucer, K.B.; Williams, R.T.; Del Ben, M.; Canning, A.; Moretti, F.; Bourret, E. Picosecond Absorption Spectroscopy of Excited States in BaBrCl with and without Eu Dopant and Au Codopant. *Physical Review Applied* **2019**, *12*, 014035. Publisher: American Physical Society, https://doi.org/10.1103/PhysRevApplied.12.014035.